Adsorption 11: 201–206, 2005

Integrating Gas Sorption with Mercury Porosimetry

SEAN P. RIGBY* AND MATTHEW J. WATT-SMITH
Department of Chemical Engineering, University of Bath, Claverton Down, Bath BA2 7AY, UK
s.p.rigby@bath.ac.uk

ROBIN S. FLETCHER
Johnson Matthey Catalysts, P.O. Box 1, Belasis Avenue, Billingham, Cleveland TS23 1LB, UK

Abstract. Previous work has shown that it is possible to use intergrated nitrogen sorption and mercury porosimetry experiments to determine the distribution of average pore length with pore diameter for mesoporous solids. In this work, the previous data analysis method has been generalised such that it is also suitable for application to samples with higher levels of mercury entrapment than before. This generalisation of the theory has facilitated the ability to use a series of progressively larger mercury scanning loops, in integrated gas sorption and porosimetry experiments, to potentially determine the full pore length distribution for pores of a given diameter, and the distribution of pore co-ordination number. The new analysis has been applied to a silica catalyst support.

Keywords: network percolation, pore length distribution

Introduction

Mesoporous silica and alumina materials are often used as supports for heterogeneous catalysts or absorbents. The transport properties of these materials influences significantly the overall performance of the catalysts based upon them. The geometry and topology of the void space determines the rate at which mass transport may occur through the pore system. Hence, techniques based upon gas sorption and/or mercury porosimetry have been developed to characterise the structure of the pore space using parameters such as the overall voidage fraction, specific (BET) surface area, specific pore volume, (BJH) pore diameter distribution, and pore connectivity. These parameters are often correlated with observed catalyst activity, and used to construct models of the porous medium within which simulations of coupled diffusion, adsorption and reaction processes, for example, may be conducted to study the effects of different pore structures on the performance of a catalyst. Pore bond network models are often used to represent the void space of porous media because it is possible to incorporate much of the void space structural complexity into them using the above characteristic parameters, while the model generally remains mathematically tractable. Pore bond networks consist of an underlying lattice structure, such as a cubic or tetrahedral lattice, where some, or all, of the edges of the lattice are occupied by pore bonds joining up the nodes. Simulations of gas/solid reactions, for example, using abstract pore bond network models have shown that the pore length distribution significantly affects the results of the simulations (Sotirchos and Zarkanitis, 1993). However, until recently (Rigby et al., 2004b), there has not been a way to determine the pore length distribution for real materials in order to be able to incorporate this characteristic of a porous medium into a pore bond network model. A method (Rigby et al., 2004b) to determine the distribution of average pore length with pore diameter has been developed which uses percolation theory to analyse the data arising from integrated gas sorption and mercury porosimetry experiments. Integrated gas sorption and mercury porosimetry experiments consist of a sequence of gas sorption or mercury porosimetry

---

*To whom correspondence should be addressed.

runs conducted in series on the same sample, by freezing entrapped mercury in place before commencing a subsequent gas sorption experiment.

Integrated gas sorption and mercury porosimetry experiments have been used to characterise the spatial distribution of different pore sizes (Rigby et al., 2004a), test for the presence of the pore-blocking effect (Rigby and Fletcher, 2004a), validate semi-empiricial alternatives to the Washburn equation (Rigby and Fletcher, 2004b), aswell as for determining the distribution of average pore length with pore diameter (Rigby et al., 2004b). It is the purpose of this paper to generalize the previous (Rigby et al., 2004b) theory and expand upon the experimental technique. Previous work (Rigby et al., 2004b) only utilized the standard mercury porosimetry experiment, consisting of a full primary mercury intrusion up to the maximum pressure possible with the apparatus and then a decrease back to ambient, and the theoretical analysis presented was only suitable for application to materials with relatively low levels of mercury entrapment. In this paper the previous theoretical analysis will be expanded so that it is also applicable to materials with higher levels of entrapment, and, in doing so, show how the distribution of pore co-ordination number might potentially be determined. This paper also describes how the extension of the experimental method to include a series of mercury porosimetry scanning loops can be used to increase the information that can be obtained about pore lengths, and even potentially determine the full distributions of pore length for each pore diameter.

Theory

In the theory presented here it is assumed that, if mercury becomes entrapped within a particular pore following porosimetry, then that pore is completely filled with mercury. It is also assumed that, if mercury retracts from a given pore, then it completely empties that pore. This type of mechanism of mercury extrusion is known as "piston-type retraction." In addition, it is also assumed that two, or more, empty pores joining at a particular common node retain direct communication between themselves via that node, and the entrapped mercury within other adjacent, but still filled, pores does not lead to a constriction causing additional pore-blocking effects. As described in detail in previous work (Rigby et al., 2004b), the validity of these assumptions for a particular sample can be tested using integrated gas sorption and mercury porosimetry. If piston-type intrusion/retraction is occurring then the BJH pore diameter distributions, derived from nitrogen adsorption isotherms obtained before and after porosimetry, will overlay each other except for pores with diameters where entrapment is occurring, in which case the pore volume of such pores will appear to decrease. If any partial intrusion or retraction is occurring then this would additionally result in the apparent creation of new small pores. The new analysis method described below also assumes that the number of nodes (vertices) in the network remains the same before and after porosimetry. This means that the network does not become separated into two disjoint sub-networks by a complete barrier of entrapped mercury.

The new analysis presented here is a substantial modification of the method to determine the distribution of average pore length with pore diameter described in earlier work (Rigby et al., 2004b). This particular analysis method (Rigby et al., 2004b) was, itself, based, in part, on the percolation analysis procedure developed by Seaton (1991). As in the Seaton (1991) method, the analysis presented here is carried out in terms of percolation variables, the values of which are calculated from pore diameter distributions (obtained from nitrogen adsorption isotherms), and the adsorption and desorption isotherms themselves. The Seaton (1991) analysis allows the determination of the pore connectivity, Z, and the lattice size, L, of a pore bond network of a porous medium. In this context, pore connectivity is defined as the mean pore co-ordination number, averaged over all of the nodes in the network. The pore co-ordination number is the number of pore bonds meeting at a given single node. Following a mercury porosimetry experiment, some of the pores may become completely filled with entrapped mercury, and are, thus, subsequently completely inaccessible to nitrogen. Hence, both the total number of open pores, T, and the connectivity of the network, Z should decline. If the connectivity, Z, is the typical open pore co-ordination number averaged over all nodes in the original empty pore network, then from the handshaking lemma for graphs (Rigby et al., 2004b):

$$(T_A/T_B) = (Z_A/Z_B) \tag{1}$$

where here, and below, subscripts B and A, refer to parameters obtained before and after porosimetry, respectively. Equation (1) assumes that the number of network nodes is a constant. However, nitrogen adsorption only allows the size distribution of accessible pores to be determined. Some pores may be free of entrapped mercury but still remain inaccessible because they are completely surrounded by filled pores. Simulations of mercury entrapment in random pore bond networks suggest that the distribution of entrapped mercury is random and homogeneous over the whole network (Androutsopoulos and Mann, 1979). Hence, percolation theory may be used to deduce the total number of open pores remaining after porosimetry, T_A, from the total number of pores directly accessible from the edge of the network, T_m, that can be measured using nitrogen adsorption, using the generalised scaling function, h, determined by Seaton (1991):

$$L^{\beta/\nu} Z_B\left(\frac{T_m}{T_B}\right) = h\left[\left(Z_B\left(\frac{T_A}{T_B}\right) - \frac{3}{2}\right)L^{1/\nu}\right] \qquad (2)$$

where β and ν are the critical scaling exponents, and have values of 0.41 and 0.88, respectively. When the level of mercury entrapment is low, and thus entrapped mercury does not disconnect any nodes, then $T_m/T_B = T_A/T_B$, as in previous work (Rigby et al., 2004b).The original percolation analysis for nitrogen sorption data developed by Seaton (1991) assumed that pore length was uncorrelated with pore diameter. However, this assumption frequently leads to inconsistencies between the decline in pore connectivity and the decline in the total number of open pores following mercury entrapment (Rigby et al., 2004a). However, if a power law relationship between the pore diameter and pore length of the form:

$$\bar{l}_i = k.d_i^{\alpha} \qquad (3)$$

where $\bar{l}_i$ is the average length of pores of diameter d_i, and k and α are parameters of the distribution, is assumed, then the decrease in pore connectivity can be reconciled with the drop in the total number of pores. This is achieved by adjusting α in the expression:

$$\frac{T_m}{T_B} = \frac{\sum_{i=1}^{N} \frac{V_{A,i}}{d_i^{(2+\alpha)}}}{\sum_{i=1}^{N} \frac{V_{B,i}}{d_i^{(2+\alpha)}}} \qquad (4)$$

where N is the number of intervals in the pore diameter distribution, and V_i is the incremental volume of pores in each size interval i, such that the experimental data satisfies Eq. (1) as closely as possible. However, the value of connectivity obtained from the percolation analysis of the nitrogen sorption isotherms obtained after mercury porosimetry, Z_m, is the average pore co-ordination number only for the part of the network remaining accessible to nitrogen. Hence, the value of pore connectivity measured in this way, Z_m, does not take into account nodes at which all pore bonds have become blocked with mercury. The distribution of pore co-ordination number amongst nodes is assumed to be completely random, and, thus, to follow a binomial distribution. Thus Z_A is related to Z_m by the expression:

$$Z_A = \left\{1 - \sum_{i=1}^{C}\left(\frac{C!}{i!(C-i)!}\right)\left(\frac{Z_B}{C}\right)^i \times \left[1 - \left(\frac{Z_B}{C}\right)\right]^{(C-i)}\left[1 - \left(\frac{T_A}{T_B}\right)\right]^i\right\} Z_m \qquad (5)$$

where C is the constant lattice bond co-ordination number of the lattice geometry upon which the pore network is based (e.g. $C = 6$ for an underlying cubic lattice, and $C = 4$ for an underlying tetrahedral lattice, and where $0 < Z_B \leq C$). From Eq. (5), when the amount of entrapped mercury is small, as in previous work (Rigby et al., 2004b), $T_A \sim T_B$, and thus $Z_A = Z_m$. Hence, it is only when the level of mercury entrapment is large, resulting in a relatively high number of totally disconnected lattice nodes, that the analysis becomes sensitive to the distribution in pore co-ordination number, and thus the underlying lattice geometry. In the fitting of the experimental sorption data from before and after porosimetry to the model, the lattice size L is also kept constant. If $(T_A/T_B).(Z_B/C)$ decreases below the percolation threshold of the underlying lattice, then the pore network will become disconnected, and L will not be a constant. Hence, there is an upper limit to the levels of mercury entrapment for which the above analysis can be applied. The pore length distribution is found by varying the fitting parameters α, Z_m, Z_B, C, and L, such that Eq. (1) is satisfied, and good fits of the experimental sorption data, from both before and after porosimetry, to the generalised scaling relation, h, are obtained. The parameter k is then obtained from:

$$k = \frac{\frac{D\tau}{L}\sum_{i=1}^{N} \frac{V_{B,i}}{d_i^{(2+\alpha)}}}{\sum_{i=1}^{N} V_{B,i}.d_i^{-2}} \qquad (6)$$

where D is the overall linear dimension of the network, and τ is the tortuosity of a pore bond. $\tau = 1$ for a regular pattern network, and $\tau = 1.1676$ for a random pattern network (Rigby et al., 2004b).

In previous work (Rigby et al., 2004b) mercury entrapment was obtained using the standard porosimetry experiment, where the mercury pressure is increased to the maximum possible value with the apparatus used (typically ∼412 MPa (60,000 psia)) and then reduced back down to ambient. This type of experiment typically entraps the maximum amount of mercury possible with the rig used. However, it is also possible to conduct experiments, typically called "scanning loops", where the pressure is only increased to some lower level below the maximum possible. This procedure generally results in lower levels of mercury entrapment. Hence, using scanning loops, it is possible to manipulate the amount and location of entrapped mercury. By conducting mercury scanning loops with successively increasing ultimate pressures it is possible to progressively increase the level of mercury entrapment. With integrated nitrogen sorption and mercury porosimetry, nitrogen sorption experiments are conducted between each separate mercury scanning loop. If samples from a given batch of porous solid are identical, then it is not necessary to conduct each integrated series, consisting of a nitrogen sorption run, followed by the mercury scanning loop, then followed by another nitrogen sorption run, on the same sample for each different ultimate mercury pressure.

In the analysis method described above the distribution of average pore length with pore diameter is found by comparing the nitrogen sorption isotherms obtained before and after the partial filling with solid mercury of the particular network being characterised. In previous work (Rigby et al., 2004b), this particular network was the original (raw) void space of the porous material with no mercury present. However, the same procedure can be performed on a material where the starting network consists, instead, of the raw pore structure already partially filled with mercury. Instead of just comparing the nitrogen sorption isotherms for the completely empty network, and the network remaining after filling some of it with mercury to an arbitrary level, to determine the average pore length distribution for the entire raw network, it is also possible to compare the sorption isotherms obtained at two different levels of partial filling with mercury, and thus obtain the average pore length distribution only for the subset of the network that was empty at the time of the first nitrogen sorption experiment in the relevant pair. In principle, the starting network could be only a tiny fraction of the original (raw) pore network of the porous solid itself (with the remainder being full of mercury), and hence the pore length distribution (α_1) obtained would be characteristic of only that small subset of the pores left empty before the last scanning loop. Once the pore length distribution is fixed for this initial subset of pores, the (potentially) different distribution for the next subset could be determined using the nitrogen sorption isotherms obtained when that next subset of pores was also free of mercury. The second pore length distribution function (α_2) would apply only to those pores filled with entrapped mercury by the second to last scanning loop, but not the last (see Fig. 1). The difference in the corresponding BJH pore diameter distributions obtained from the nitrogen adsorption isotherms measured before and after each mercury scanning loop would determine to what volume of which diameter pores the second length distribution function applied. In principle (depending on the degree of pore shielding), the resolution of the method could be made almost arbitrarily small by using mercury scanning loops with ever closer ultimate pressures to only marginally change the amount of pore space blocked with entrapped mercury each time. Hence, using a series of integrated experiments with a sequence of scanning loops, the pore length distribution for pores of a particular diameter could be deduced. The resolution of the distribution would increase as the maximum level of mercury entrapment possible for the material increased. It is this second type of experiment which will be demonstrated here. The determination of the distribution of pore coordination number will be demonstrated in a subsequent publication.

Results and Discussion

The more general experimental procedure used here is the same as that described in previous work (Rigby et al., 2004b). The sample studied in this work is a silica catalyst support pellet denoted W1. For samples from batch W1, nitrogen sorption isotherms, denoted 1, 2 and 3, were obtained after each of mercury scanning loops up to ultimate pressures of 0 MPa (i.e. fresh sample), 275 MPa and 412 MPa, respectively. Only two scanning loops were used in this work due to the relatively low level of mercury entrapment for batch W1, and to simply demonstrate the operation of the method. The level of mercury entrapment was found to increase with the ultimate pressure of the scanning loop and was validated by weighing the sample. A set of typical isotherms is shown in Fig. 1(a). It can be seen that the pore volume accessible to nitrogen decreases with higher ultimate mercury scanning loop pressures due to increased mercury entrapment. The BJH cumulative pore diameter distributions obtained

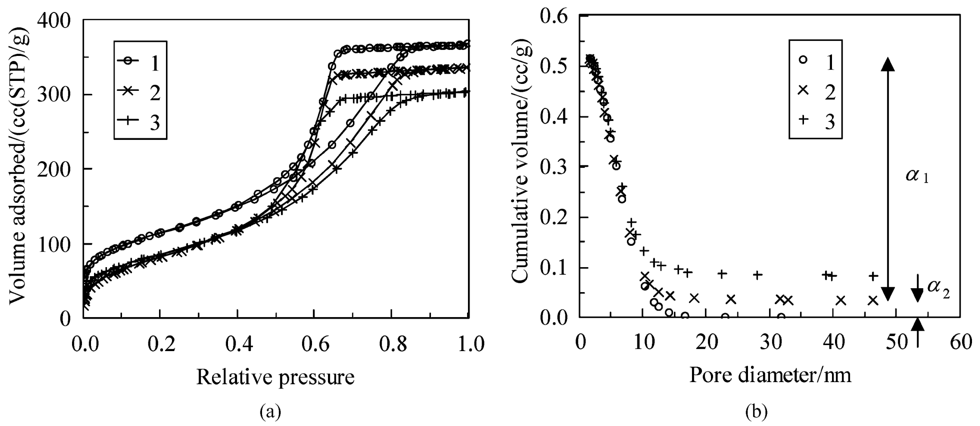

(a) (b)

Figure 1. (a) Nitrogen sorption isotherms, and (b) BJH cumulative pore diameter distributions, obtained for a fresh sample (1), and after mercury porosimetry scanning loops to (2) 275 MPa and (3) 412 MPa.

from the adsorption isotherms shown in Fig. 1(a) are shown in Fig. 1(b). In the case of the distributions obtained after mercury entrapment, the ultimate cumulative volumes have been renormalised to that obtained for a fresh sample. This method of presenting the data demonstrates that the pore diameter distributions obtained after mercury entrapment are identical to that obtained for a fresh pellet, within experimental error, at smaller pore diameters, but differ at larger pore diameters. As more mercury becomes entrapped, more larger pores become inaccessible to nitrogen. The data in Fig. 1(b) suggests that mercury intrusion and retraction occurs by a piston-type mechanism, as required for the analysis method. The incremental pore diameter distribution for pores filled with entrapped mercury by the 276 MPa scanning loop, but not the 414 MPa loop, (Group 2) is shown in Fig. 2, along with that for the remainder of the pores (Group 1), and that for the complete set of all pores.

The nitrogen sorption isotherms in Fig. 1 were analysed using the above analysis, utilising the limiting versions of Eqs. (2) and (5) applicable to low levels of mercury entrapment. The fits of the data to the generalised scaling relation (Seaton, 1991) are shown in Fig. 3. The best fit parameters obtained from the analysis are shown in Table 1. The values of α_1 and α_2 for pores in Groups 1 and 2 are -1.0 and -0.9, respectively. Hence, since these values are slightly different, there is likely to be a distribution of pore lengths for pores of a given diameter within pellets from batch W1.

Table 1. Fitted parameters (subscripts refer to the relevant isotherms).

Z_1	Z_2	Z_3	Z_2/Z_1	Z_3/Z_2	T_2/T_1	T_3/T_2	L
3.4	3.3	3.0	0.971	0.909	0.973	0.908	9.5

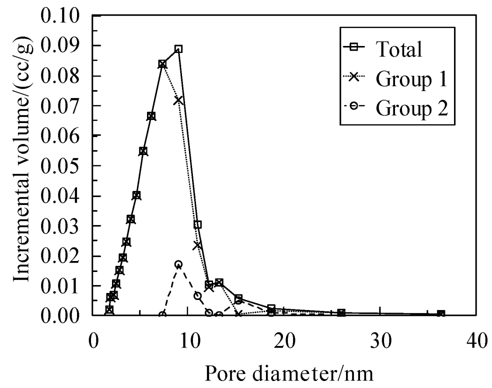

Figure 2. Incremental pore diameter distributions.

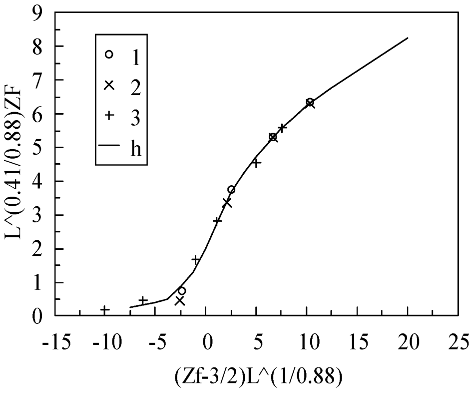

Figure 3. Fits of the nitrogen sorption data in Fig. 1 to h.

Conclusions

The extension of the experimental method previously utilized in integrated gas sorption and mercury porosimetry to include porosimetry scanning loops has been demonstrated. Using this expanded type of experiment, it has been shown that increased information on the distribution of pore length with diameter, beyond simply the variation in the average length of pores of a given diameter, can be obtained.

References

Androutsopoulos, G.P. and R. Mann, "Evaluation of Mercury Porosimeter Experiments Using a Network Pore Structure Model," *Chem. Engng Sci.*, **34**, 1203–1212 (1979).

Rigby, S.P. and R.S. Fletcher, "Experimental Evidence for Pore Blocking as the Mechanism for Nitrogen Sorption Hysteresis in a Mesoporous Material," *J. Phys. Chem. B*, **108**, 4690–4695 (2004a).

Rigby, S.P. and R.S. Fletcher, "Interfacing Mercury Porosimetry with Nitrogen Sorption," *Part. Part. Syst. Charac.*, **21**, 138–148 (2004b).

Rigby, S.P., R.S. Fletcher, and S.N. Riley, "Characterisation of Porous Solids Using Integrated Nitrogen Sorption and Mercury Porosimetry," *Chem. Engng Sci.*, **59**, 41–51 (2004a).

Rigby, S.P., M.J. Watt-Smith, and R.S. Fletcher, "Simultaneous Determination of the Pore Length Distribution and Pore Connectivity for Porous Catalyst Supports Using Integrated Nitrogen Sorption and Mercury Porosimetry," *J. Catal.*, **227**, 68–76 (2004b).

Seaton, N.A., "Determination of the Connectivity of Porous Solids from Nitrogen Sorption Measurements," *Chem. Engng Sci.*, **46**, 1895–1909 (1991).

Sotirchos, S.V and S. Zarkanitis, "A Distributed Pore Size and Length Model for Porous Media Reacting with Diminishing Porosity," *Chem. Engng Sci.*, **48**, 1487–1502 (1993).